

# Visualization of Secondary Flow in an Inclined Double-Inlet Pulse Tube Refrigerator

M. Shiraishi<sup>1</sup>, M. Murakami<sup>2</sup>, A. Nakano<sup>3</sup> and T. Iida<sup>3</sup>

<sup>1</sup>National Institute of AIST  
Tsukuba 305-8564 Japan

<sup>2</sup>University of Tsukuba,  
Tsukuba 305-8573 Japan

<sup>3</sup>Orbital-Engineering Co.,  
Yokohama 221-0822 Japan

## ABSTRACT

Secondary flow in an inclined double-inlet pulse tube refrigerator at typical inclination angles of  $0^\circ$  to  $180^\circ$  was studied by using a smoke-wire flow visualization technique. Results revealed that gravity-driven convective secondary flow were induced and the overall convective secondary flow in the pulse tube was formed by the superposition of this gravity-driven flow on acoustic streaming and on DC flow inherent in a double-inlet pulse tube refrigerator. Even if the cold end was lower than the hot end, the overall secondary flow was affected by gravity. Results also revealed that the flow behavior of gravity-driven flow in the double-inlet pulse tube was the same as that previously reported for an inclined orifice pulse tube refrigerator, although the gravity-driven flow in a double-inlet pulse tube had a more direct effect on the cooling performance as compared to an inclined orifice pulse tube.

## INTRODUCTION

The cooling performance of an orifice pulse tube refrigerator is sensitive to the inclination angle ( $\theta$ ) of the refrigerator, especially when  $\theta > 60^\circ$ .<sup>1,2,3</sup> Here, we defined  $\theta = 0^\circ$  as the vertical position with the cold end lower than the hot end (see inset of Fig. 1). For example 1, the lowest temperature of the cold end at  $\theta = 120^\circ$ , without a heat load, increases to about 3 times that at  $\theta = 0^\circ$ . In a previous study, we used a smoke-wire flow visualization technique to observe the secondary flow in an inclined orifice pulse tube refrigerator.<sup>4,5</sup> We found that when  $\theta > 0^\circ$ , a gravity-driven convective secondary flow (hereafter called gravity-driven flow) is newly induced in the pulse tube, in addition to acoustic streaming, which is a secondary flow inherent in pulse tubes due to pressure oscillation independent of  $\theta$ .<sup>6</sup> These visualization results showed that the overall secondary flow (hereafter called overall flow) in an inclined orifice pulse tube refrigerator is formed by superposition of gravity-driven flow on acoustic streaming. Moreover, the effect of  $\theta$  on cooling performance is well explained by the change in convective heat loss caused by the overall flow in a pulse tube.

The cooling performance of a double-inlet pulse tube refrigerator is also sensitive to  $\theta$ , and this effect causes serious problems for practical applications.<sup>7,8,9</sup> Based on previous results for an orifice pulse tube,

gravity-driven flow might be also be induced in a double-inlet pulse tube when  $\theta > 0^\circ$ , although the flow behavior of the overall flow might differ from an orifice pulse tube. The difference in flow behavior arises because DC flow is induced and two kinds of secondary flow are inherent in a double-inlet pulse tube independent of  $\theta$ : a) acoustic streaming similar to that in an orifice pulse tube, and b) DC flow, which never occurs in an orifice pulse tube.<sup>10</sup> When a double-inlet pulse tube is at an inclined position, the overall flow might be formed by superposition of the gravity-driven flow on the acoustic streaming and DC flow. The behavior of overall flow in an inclined double-inlet pulse tubes has not been clarified in detail yet. Questions remain about whether gravity-driven flow occurs or not, and about the behavior of overall flow in the pulse tube when the pulse tube is in an inclined position.

The objective of this study was to observe the secondary flow in an inclined double-inlet pulse tube refrigerator and to clarify gravity-driven flow and the behavior of overall flow by using a smoke-wire flow visualization technique.

## EXPERIMENT

Figure 1 shows a schematic of the apparatus used to visualize the flow in a double-inlet pulse tube refrigerator. The pulse tube was made with a transparent plastic tube for visualization, and was 16 mm in inner diameter and 320 mm long. The regenerator was composed of a pile of #100 stainless steel screens, was 18 mm in outer diameter and 170 mm long, and its warm end was connected to a rotary valve. The reservoir was a plastic vessel with a volume about 6 times larger than the pulse tube and was connected to the pulse tube via an orifice valve (Nupro, type BM). The bypass line connected the inlet of the regenerator and the hot end of the pulse tube via a bypass valve installed near the hot end. The arrow (imprinted on the side of valve), indicating the direction of flow suggested by the manufacturer, was directed toward the hot end, as shown in the figure. The valve was fully open after 6 turns, and each turn was graduated into 25 divisions. The valve opening was expressed in turn-divisions as arbitrary units; at 150 turn-divisions, the valve was fully open. Tube fittings were installed at three locations along the pulse tube: to fix a smoke-wire (located at the middle point between the cold and hot ends), two thermocouples (one each at the cold and hot ends), and a pressure transducer (at the hot end). The smoke-wire was a 0.1 mm diameter tungsten wire. Both ends of the smoke-wire were soldered to copper supports, which acted both as electrodes and as supports to keep the wire taut. Chromel-Almel sheathed thermocouples were installed at the cold end and hot end to measure the gas temperature. The performance of the refrigerator was estimated from the difference in gas temperature. In general, the larger temperature difference produces a better performance. Three pressure transducers (strain gauge type) were installed near the inlet of the regenerator, at the hot end of the pulse tube, and in the reservoir, respectively. The pulse tube refrigerator was fixed on a base stand that had a rotatable horizontal axle in order to rotate the refrigerator from a vertical position ( $\theta = 0^\circ$ ) to an inverted position ( $\theta = 180^\circ$ ). The pressure oscillation of air as a working gas was generated by introducing pressurized air at about 0.2 MPa into a rotary valve and then releasing it into the atmosphere.

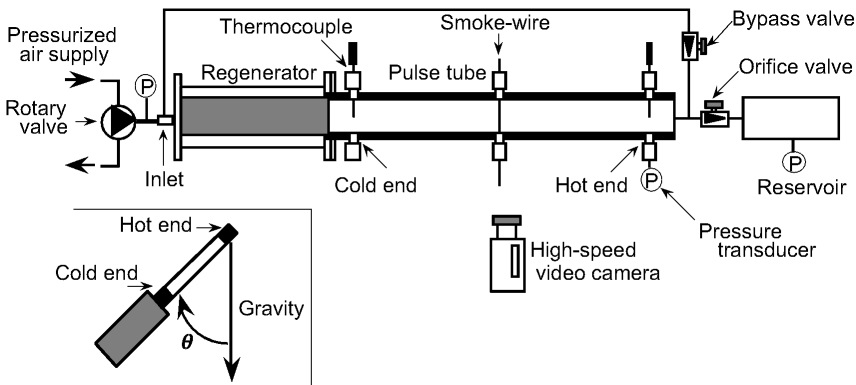


**Figure 1.** Schematic of experimental apparatus used to visualize convective secondary flow in an inclined pulse tube refrigerator. Inset shows definition of inclination angle  $\theta$ .

Experimental conditions suitable for visualization were determined based on the results of preliminary and previous experiments.<sup>5</sup> The frequency was 6 Hz, and the amplitude of the pressure wave defined as the compression ratio between the high and low pressure at the inlet of regenerator was 1.2. The openings of the orifice and the bypass valve were then determined to maximize the difference in gas temperature between the cold end and the hot end to the optimum condition for the refrigerator in a vertical position ( $\theta = 0^\circ$ ). The opening of the orifice valve was adjusted to 15 turn-divisions by closing the bypass valve, and while keeping the opening of the orifice valve at 15 turn-divisions, the opening of the bypass valve was adjusted to 5 turn-divisions. These openings were then fixed at the respective values throughout the experiment. After the smoke-wire surface was coated with paraffin, the wire was fixed inside the pulse tube. The lead wires of the smoke-wire were connected to a high-voltage pulse generator and the pressure oscillations were then introduced into the refrigerator. After steady state was confirmed by monitoring the gas temperature, a smoke-line was emitted just at the moment when gas started to move toward the hot end after the compression process was started. The movement of the smoke-line was recorded with a high-speed video camera at a rate of 400 frames/sec over 5 cycles of oscillation.

The visualization was repeated at  $\theta = 0^\circ, 60^\circ, 90^\circ, 120^\circ, 150^\circ$  and  $180^\circ$ .

## RESULTS AND DISCUSSION

The refrigerator in this study was designed for visualization, and the temperature difference between the cold end and hot end was roughly one order of magnitude smaller than for a conventional pulse tube refrigerators in practical applications. Prior to visualization, the performance of the refrigerator, which can be characterized by the gas-temperature difference between the cold end and the hot end, was measured to confirm the effect of  $\theta$  under the same conditions used in the visualization. Figure 2 shows the measured temperature difference. The temperature difference decreased with increasing  $\theta$ , then reached a minimum, and finally slightly increased at  $\theta = 180^\circ$ . Even though the change in temperature difference as a function of  $\theta$  is significantly smaller than that in practical applications, the dependence of cooling performance on  $\theta$  is the same; namely, with increasing  $\theta$ , the temperature difference decreased until  $\theta = 150^\circ$  and, then slightly increased at  $\theta = 180^\circ$ . This dependence suggests that the effect of  $\theta$  occurs under the adjusted conditions and that this effect is non-negligible.

Figure 3 shows the typical visualization results for the oscillation of the smoke-line during the first two cycles of oscillation as representative results for all five cycles. The smoke-line was emitted at the moment when gas started to move toward the hot end after the compression process was started. After the smoke-line was emitted, it moved toward the hot end (toward the top of each frame) and then returned to its original position at the smoke-wire, until the next oscillation started. Frame 1 shows the smoke-line just after being emitted from the smoke-wire, namely, the smoke line is at almost the same position as the smoke-wire itself. Frames 3 and 5 show the smoke-line at the turning point where the smoke-line changes its direction of motion, namely, from the direction of the hot end to the direction of the cold end (Frame 3), called the hot-end turning point, and from the direction of the cold end to the direction of the hot end

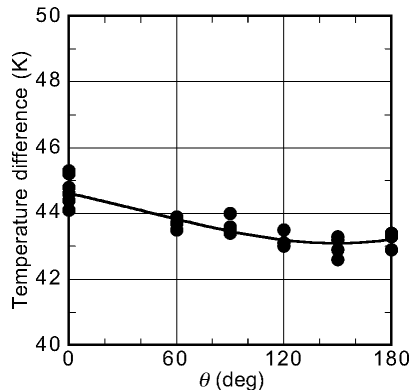


**Figure 2.** Measured difference in gas temperature between the hot and cold ends of an inclined pulse tube refrigerator as a function of inclination angle,  $\theta$ .

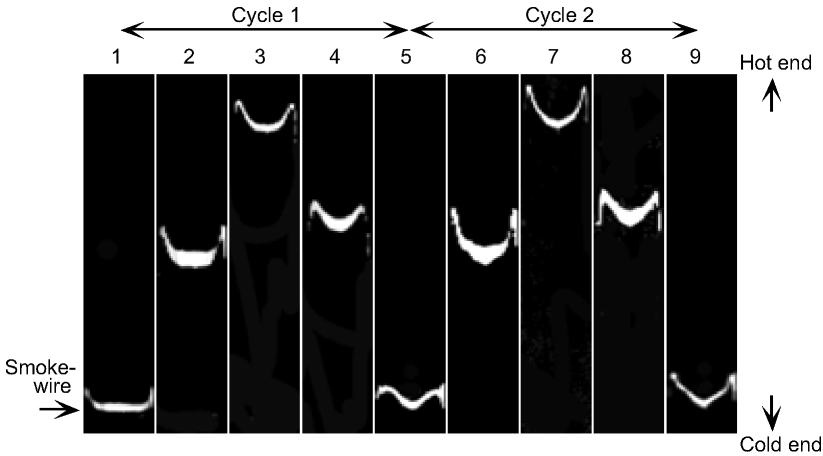


**Figure 3.** Typical visualization results of a pulse tube inclined at inclination angle  $\theta = 0^\circ$ . The smoke line was emitted at the moment when gas started to move toward the hot end. Frame 1 shows the smoke-line just after being emitted from the smoke-wire. Frames 3 and 5 show the smoke-line at the turning point where the smoke-line changes its direction of motion, and Frames 2 and 4 show the smoke-line passing through the halfway point between the turning points.

(Frame 5), called the cold-end turning point. Frames 2 and 4 show the smoke-line passing through the halfway point between the hot end and cold end turning points. The behavior evident in these five frames is the same as that in the next cycle of oscillation. Although details of the smoke-line profiles depended on  $\theta$ , the major feature in the smoke-line behavior is that the oscillating main flow in the pulse tube was accompanied by a secondary flow. The oscillating smoke-line gradually elongated in the axial direction as evidenced by the distance between the leading edge of the smoke-line in the core region of pulse tube and that near the wall. This elongation of the smoke-line is due to the secondary flow.

To investigate the effect of  $\theta$  on the secondary flow, we compared the change in the shape of the smoke-line at the hot-end turning point (such as Frames 3 and 7 in Fig. 3), assuming that the change before and after a cycle is due only to secondary flow. Figure 4 shows a summarized result for  $\theta = 0^\circ, 90^\circ, 150^\circ$  and  $180^\circ$  for cycles 1, 3 and 5. When  $\theta = 0^\circ$  (the pulse tube was vertical), the smoke-line in the core region remained near the position of the first cycle, while the smoke-line near the wall was elongated toward the hot end. When  $\theta = 0^\circ$ , only two kinds of secondary flow were present in the pulse tube: (a) acoustic streaming, where the fluid goes toward the cold end in the core region, and the associated return flow goes toward the hot end along the peripheral wall, and (b) DC flow, where the fluid goes toward the hot end with a parabolic velocity profile similar to that of Poiseuille flow in a tube.<sup>11</sup> Because the refrigerator was adjusted to the optimum condition, the DC flow was counterbalanced by the acoustic streaming in the core region and the overall flow in the core region was reduced to almost zero so that the smoke line in the core region remained near the initial position of the first cycle.<sup>11</sup> Both the DC flow and acoustic streaming near the wall travel toward the hot end, thus causing the velocity of the flow near the wall to increase so that the smoke-line near wall was elongated toward the hot end. When  $\theta = 90^\circ$  or  $150^\circ$ , the shape of the smoke-line was deformed from symmetric when  $\theta = 0^\circ$  to asymmetric. Moreover, the leading edge of the smoke-line in the core region drifted toward the upper side wall and also toward the cold end. The drift toward the cold end at  $150^\circ$  was larger than that at  $90^\circ$ . When  $\theta = 180^\circ$ , the shape of the smoke-line once again became symmetric, similar to the smoke-line at  $\theta = 0^\circ$ , although the leading edge of the smoke-line in the core region drifted toward the cold end.

To further evaluate the overall flow, we digitized the smoke-lines in Fig. 4 by using an image processing system. Figure 5 shows the smoke-lines of cycles 1 and 5 as representative cycles. The difference in the overall positions between two smoke-lines at a given position is considered the average movement during two successive cycles as a result of overall secondary flow. Based on Fig. 5, a secondary flow in the pulse tube occurred for all  $\theta$ , but had two different flow patterns depending on  $\theta$ . When  $\theta = 0$  or  $180^\circ$ , the pattern was concentric, whereas when  $\theta = 60^\circ \sim 150^\circ$ , the pattern was a continuous single loop. In the

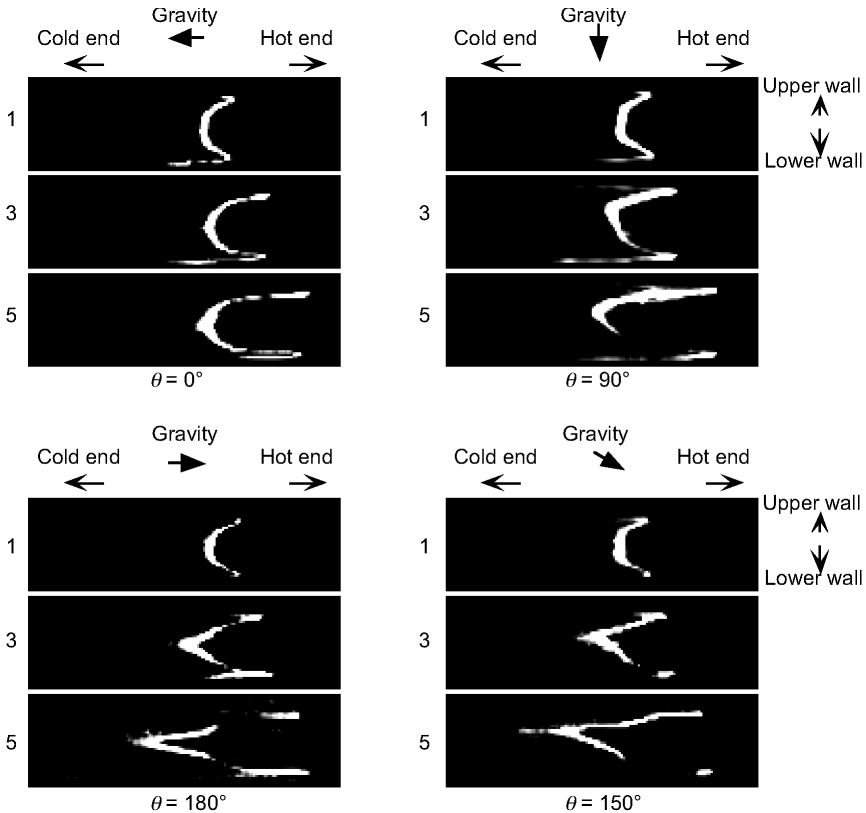


**Figure 4.** Comparison of smoke-lines at inclination angle  $\theta = 0^\circ, 90^\circ, 150^\circ$  and  $180^\circ$  for the smoke-line at the hot-end turning point (such as Frames 3 and 7 in Fig. 3) of three representative cycles (1, 3, and 5)

concentric pattern, when  $\theta = 180^\circ$ , the fluid flowed to the cold end in the core region and returned to the hot end along the peripheral wall, whereas when  $\theta = 0^\circ$ , only the fluid near the peripheral wall flowed to the hot end and the fluid in the core region stayed at the initial position. In the continuous single-loop pattern, the fluid flowed to the cold end along the upper side-wall of the pulse tube and returned to the hot end along the lower side-wall. Even if  $\theta = 60^\circ$ , the flow pattern differed from that when  $\theta = 0^\circ$  because the leading edge of the smoke-line in the core region shifted toward the cold end and slightly toward the upper side-wall with time. Figure 5 clearly reveals the major features of the flow behavior caused by the occurrence of gravity-driven flow in an inclined pulse tube refrigerator.<sup>5</sup>

From the digitized smoke-lines, we estimated the velocity profile of the overall flow by using the change in the relative position of the smoke-line before and after a cycle by assuming that the change was due only to overall secondary flow. The velocity profiles obtained were an average profile for a cycle. Figure 6 shows these velocity profiles as a function of  $\theta$ . Comparison of the profiles clearly reveals that the profiles for  $\theta = 0^\circ$  and  $180^\circ$  were nearly symmetric with respect to the axis of the pulse tube, whereas those for  $\theta = 90^\circ$  and  $150^\circ$  were asymmetric with the leading edge of the velocity profile in the core region drifted toward the upper side-wall. The symmetric and asymmetric profiles correspond to the concentric and continuous single-loop flow patterns, respectively. In this experiment, the velocity of the overall flow in the core region at  $\theta = 180^\circ$  was about 30 mm/s. In a previous study of an inclined orifice pulse tube refrigerator, the velocity at  $\theta = 180^\circ$  was about 60 mm/s, which is two times faster.<sup>5</sup> This difference in the velocity can be explained as follows: In an orifice pulse tube, the velocity of the gravity-driven flow in the core region is superimposed on the velocity of the acoustic streaming (about -25 mm/s), whereas in a double inlet pulse tube, it is superimposed on the secondary flow with almost zero velocity due to the counterbalance between acoustic streaming and DC flow. Therefore, in an inclined double-inlet pulse tube,

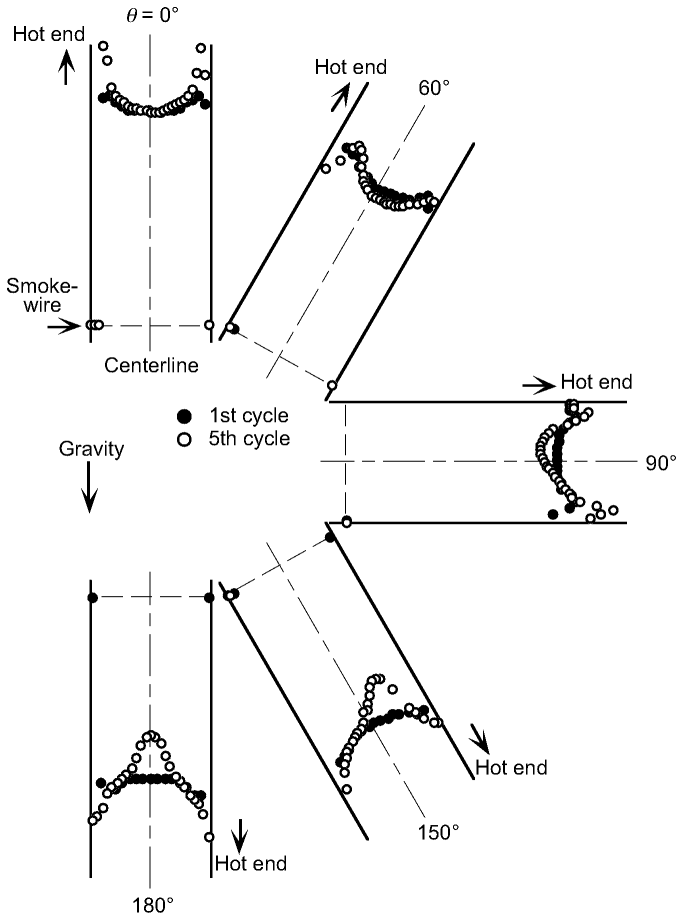


**Figure 5.** Smoke-lines for two representative cycles (1 and 5) digitized from photos in Fig. 4 by using an image processing technique. Inclination of each plot corresponds to the inclined position  $\theta$ .

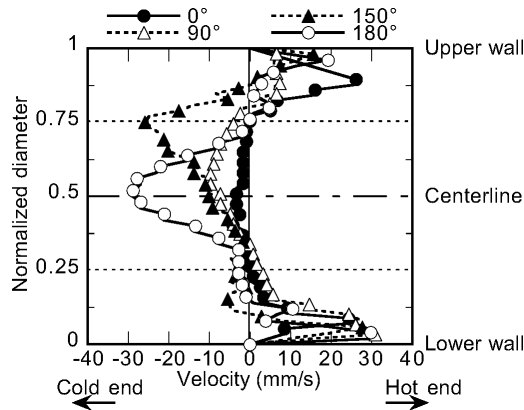


**Figure 6.** Velocity profiles of secondary flow estimated from the change in relative position of the smoke-line before and after a cycle. Positive velocity corresponds to the flow towards the hot end, and negative to the cold end. Upper and lower walls correspond to upper and lower side-walls of the pulse tube at inclined positions of inclination angle  $\theta = 90^\circ$  and  $150^\circ$ .

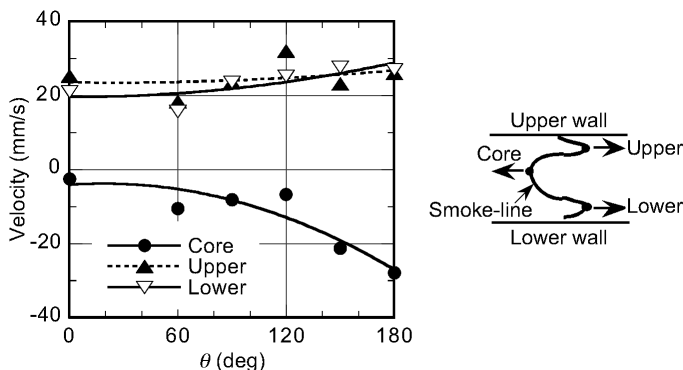


**Figure 7.** Velocities of the leading edges of a smoke-line as a function of inclination angle  $\theta$ . Core, Upper, and Lower correspond to the leading edges in the core region, near the upper wall, and near the lower wall, respectively, as shown in the illustration.

the velocity of the overall flow in the core region is almost equal to that of the gravity driven flow so that the velocity is always affected by gravity-driven flow. On the other hand, the velocity in an inclined orifice pulse tube is not always affected by only gravity-driven flow because the velocity is determined from the superposition of gravity-driven flow on acoustic streaming.

Figure 7 shows the velocities of three representative leading edges (see illustration of the figure) on a smoke-line estimated from the digitized smoke-lines. The velocity of the leading edge in the core region (core) was nearly zero at  $\theta = 0^\circ$  because the DC flow was counterbalanced by the acoustic streaming in the core region, and the overall flow was reduced to almost zero. With increasing  $q$ , the velocity toward the cold end (negative velocity) increased due to gravity-driven flow and reached about 30 mm/s at  $\theta = 180^\circ$ . In contrast, velocities of the leading edges near both the upper and lower walls were about 20 mm/s at  $\theta = 0^\circ$  due to superposition of the DC flow and acoustic streaming near the wall. Even when gravity-driven flow was induced at  $\theta > 0$ , the velocities of the leading edges only slightly increased with increasing  $\theta$ .

## SUMMARY

Secondary flow in an inclined double-inlet pulse tube refrigerator was clarified by using a smoke-wire flow visualization technique. Results revealed when  $\theta > 0^\circ$ , a gravity-driven convective secondary flow was induced, and even if the inclination angle was less than  $90^\circ$  (i.e., the cold end was lower than the hot end), the overall flow was affected by gravity. In conclusion, the gravity-driven flow in a double-inlet pulse tube has a more direct effect on the cooling performance compared to that in an inclined orifice pulse tube.

## REFERENCES

1. Thummes, G., Schreiber, M., Landgraf, R. and Heiden, C., "Convective Heat Losses in Pulse Tube Coolers: Effect of Pulse Tube Inclination," *Cryocoolers 9*, Plenum Press, New York (1997), pp. 393-402.
2. Johnson, D. L., Collins, S. A., Heun, M. K., Ross, Jr., R. G. and Kalivoda, C., "Performance Characterization of the TRW 3503 and 6020 Pulse Tube Coolers," *Cryocoolers 9*, Plenum Press, New York (1997), pp. 183-193.
3. Hiratsuka, Y., Murayama, K., Maeda, Y., Imai, F., Kang, K. Y. and Matsubara, Y., "Development of a Long-Life Stirling Pulse Tube Cryocooler for a Superconducting Filter Subsystem," *Cryocoolers 11*, Kluwer Academic/Plenum Publishers, New York (2001), pp. 119-124.
4. Shiraishi, M., Takamatsu, K., Murakami, M. and Nakano, A., "Visualization Study of Secondary Flow in an Inclined Pulse Tube Refrigerator," *Adv. in Cryogenic Engineering*, Vol. 45B, Kluwer Academic/Plenum Publishers, New York (2000), pp. 119-125.

5. Shiraishi, M., Takamatsu, K., Murakami, M. and Nakano, A., "Dependence of Convective secondary flow on inclination angle in an inclined pulse tube refrigerator revealed by visualization," *Cryogenics*, Vol.44, Issue: 2 (February 2004), pp. 101-107.
6. Olson, J. R. and Swift, G. W., "Suppression of Acoustic Streaming in Tapered Pulse Tube," *Cryocoolers 10*, Plenum Publishing Corp., New York (1999), pp. 307-313.
7. Kasthuriangan, S., Jacob, S., Karunanithi, R., Behera, U. and Nadig, D. S., "Experimental Studies of Convection in a Single Stage Pulse Tube Refrigerator," *Adv. in Cryogenic Engineering*, Vol. 49B, Amer. Institute of Physics, Melville, NY (2004), pp. 1474-1481.
8. Wang, C. and Gifford, P. E., "Single-Stage Pulse Tube Cryocooler for Horizontally Cooling HTS MRI Probe", *Adv. in Cryogenic Engineering*, Vol. 49B, Amer. Institute of Physics, Melville, NY (2004), pp. 1805-1811.
9. Wang, C., "Efficient 10 K Pulse Tube Cryocoolers," *Cryocoolers 13*, Kluwer Academic/Plenum Publishers, New York (2005), pp. 133-140.
10. Gedeon, D., "DC Gas Flows in Stirling and Pulse Tube Cryocoolers," *Cryocoolers 9*, Plenum Press, New York (1997), pp. 385-392.
11. Shiraishi, M., Takamatsu, K., Murakami, M., Nakano, A., Iida, T. and Hozumi, Y., "Visualization of DC Gas Flows in a Double-Inlet Pulse Tube Refrigerator with a Second Orifice Valve", *Cryocoolers 11*, Kluwer Academic/Plenum Publishers, New York (2001), pp. 371-379.